The EMBO Journal (2009) 28, 3613–3622 | © 2009 European Molecular Biology Organization | All Rights Reserved 0261-4189/09
www.embojournal.org

THE EMBO JOURNAL

Structural basis of phosphodiesterase 6 inhibition by the C-terminal region of the γ-subunit

Brandy Barren[1], Lokesh Gakhar[2], Hakim Muradov[1], Kimberly K Boyd[1], S Ramaswamy[1,2,3] and Nikolai O Artemyev[1,*]

[1]Department of Molecular Physiology and Biophysics, University of Iowa, Iowa City, IA, USA and [2]Department of Biochemistry, University of Iowa, Iowa City, IA, USA

The inhibitory interaction of phosphodiesterase-6 (PDE6) with its γ-subunit (Pγ) is pivotal in vertebrate phototransduction. Here, crystal structures of a chimaeric PDE5/PDE6 catalytic domain (PDE5/6cd) complexed with sildenafil or 3-isobutyl-1-methylxanthine and the Pγ-inhibitory peptide $P\gamma_{70-87}$ have been determined at 2.9 and 3.0 Å, respectively. These structures show the determinants and the mechanism of the PDE6 inhibition by Pγ and suggest the conformational change of Pγ on transducin activation. Two variable H- and M-loops of PDE5/6cd form a distinct interface that contributes to the Pγ-binding site. This allows the Pγ C-terminus to fit into the opening of the catalytic pocket, blocking cGMP access to the active site. Our analysis suggests that disruption of the H–M loop interface and Pγ-binding site is a molecular cause of retinal degeneration in *atrd3* mice. Comparison of the two PDE5/6cd structures shows an overlap between the sildenafil and $P\gamma_{70-87}$-binding sites, thereby providing critical insights into the side effects of PDE5 inhibitors on vision.

The EMBO Journal (2009) **28,** 3613–3622. doi:10.1038/emboj.2009.284; Published online 1 October 2009
Subject Categories: signal transduction; structural biology
Keywords: phosphodiesterase 6; phototransduction; transducin; X-ray crystallography

Introduction

Phosphodiesterases (PDEs) of cyclic nucleotides are major enzymes modulating cellular levels of cAMP and cGMP. Eleven class I PDE families, PDE1–11, have been identified in mammalian tissues based on their sequence homology, substrate selectivity, and regulation (Conti and Beavo, 2007; Francis *et al*, 2009). The PDE6 family of enzymes serves as central effectors in the visual transduction cascade in cone and rod photoreceptors. The effector function of PDE6 is critically supported by the unique inhibitory γ-subunit (Pγ). In dark-adapted rods, two copies of Pγ block activity of the PDE6 catalytic heterodimer PDE6AB. In cones, cone-specific Pγ inhibits homodimeric PDE6C. On light stimulation, marked activation of PDE6 occurs when the activated α-subunit of the visual G-protein transducin, $G\alpha_t$-GTP, binds to Pγ and relieves its inhibition of PDE6 (Arshavsky *et al*, 2002; Lamb and Pugh, 2006; Fu and Yau, 2007).

Each PDE6 subunit in the catalytic dimer is composed of three structural domains: two N-terminal regulatory GAF domains (GAFa and GAFb) and the conserved C-terminal PDE catalytic domain (Cote, 2004; Conti and Beavo, 2007; Francis *et al*, 2009). A general map of the Pγ-PDE6 interactions has been defined in biochemical studies. Two regions of Pγ are primarily involved in the interaction with the PDE6 catalytic subunits, the proline-rich polycationic region (residues 24–45 of rod Pγ) and the Pγ C-terminus (Pγ-residues 74–87) (Artemyev and Hamm, 1992; Skiba *et al*, 1992; Takemoto *et al*, 1992; Artemyev *et al*, 1996; Granovsky *et al*, 1997; Mou and Cote, 2001; Muradov *et al*, 2001; Guo *et al*, 2006). The polycationic region of Pγ binds to the PDE6 GAFa domain and importantly contributes to the overall affinity of Pγ for PDE6 catalytic subunits. The C-terminus of Pγ constitutes the key inhibitory domain. It interacts with the PDE6 catalytic domain and occludes the active site (Artemyev *et al*, 1996; Granovsky *et al*, 1997). Despite the wealth of structural information developed for the PDE catalytic domains from many of the 11 families, structural data on the PDE6 catalytic domain and its interaction with Pγ are lacking (Conti and Beavo, 2007; Francis *et al*, 2009). The failure of functional expression of PDE6 in various systems has impeded the understanding of the structural basis of PDE6 function (Qin and Baehr, 1994; Granovsky *et al*, 1998; Liu *et al*, 2004). Tangible progress has been achieved through characterization of chimaeric enzymes between PDE6 and the related PDE5 enzyme, which is readily attainable as recombinant protein (Granovsky *et al*, 1998; Granovsky and Artemyev, 2000, 2001a). PDE5 and PDE6 share a common domain organization, considerable homology of the catalytic domains, specificity for cGMP relative to cAMP, and sensitivity to common catalytic-site inhibitors (Cote, 2004; Conti and Beavo, 2007; Francis *et al*, 2009). An important difference between the two PDE families is that PDE5 is not inhibited by Pγ (Granovsky *et al*, 1998). Only very limited PDE6 sequences seem to be allowed in bacterially expressed chimaeric PDE5/6 catalytic domains retaining enzymatic activity (Muradov *et al*, 2006). Nonetheless, a replacement of the M-loop/α-helix 15 region in the bovine PDE5 catalytic domain with the corresponding sequence of bovine PDE6C yielded a fully functional chimaera C6 that was potently inhibited by Pγ or the Pγ C-terminal peptide, $P\gamma_{63-87}$ (Muradov *et al*, 2006).

To study the PDE6–Pγ interactions and the Pγ-inhibitory mechanism by X-ray crystallography, we have generated a C6 equivalent chimaera (termed PDE5/6cd) based on the sequences of human PDE5 and PDE6. Two structures of PDE5/6cd have been solved: (1) in complex with sildenafil (Viagra) and (2) in complex with 3-isobutyl-1-methylxanthine (IBMX) and the Pγ-inhibitory peptide, $P\gamma_{70-87}$. These structures

*Corresponding author. Department of Molecular Physiology and Biophysics, University of Iowa, 51 Newton Road, 5-532 BSB, Iowa City, IA 52242, USA. Tel.: +1 319 335 7864; Fax: +1 319 335 7330; E-mail: nikolai-artemyev@uiowa.edu
[3]Present address: Institute for Stem Cell Biology and Regenerative Medicine, Bangalore, India

Received: 3 August 2009; accepted: 24 August 2009; published online: 1 October 2009

yield important molecular details on the interaction of the Pγ C-terminus with the PDE6 catalytic subunits and the relationships between the Pγ- and drug-binding sites at the catalytic pocket. Furthermore, a novel interface is revealed between the PDE H- and M-loops that is essential for Pγ binding. Mutation Asn^{605}Ser in PDE6B causes atypical retinal degeneration 3 (*atrd3*) in mice (Thaung *et al*, 2002; Hart *et al*, 2005). The corresponding Asn residue in the PDE5/6cd structures is a critical element of the H/M-loop interface and the Pγ-binding site. Our analysis suggests that impaired inhibition of PDE6 by Pγ is the underlying mechanism of *atrd3*.

Results

Characterization of the chimaeric PDE5/6 catalytic domain, PDE5/6cd

Our original Pγ-sensitive PDE5/6 chimaeric catalytic domain C6 was prepared using bovine PDE5 and PDE6C sequences (Muradov *et al*, 2006). All known atomic structures of the PDE5 catalytic domain have been solved using the sequence of human PDE5 (Sung *et al*, 2003; Card *et al*, 2004; Huai *et al*, 2004; Zhang *et al*, 2004; Wang *et al*, 2006). Therefore, a new construct was generated based on the human PDE5 and PDE6 sequences (Figure 1). This chimaeric PDE5/6 catalytic domain, PDE5/6cd, was readily expressed in *Escherichia coli* as a highly soluble and functional protein. Purified PDE5/6cd was analysed for enzymatic activity and the ability to interact with Pγ and the inhibitory Pγ peptides, $P\gamma_{63-87}$ and $P\gamma_{70-87}$. The K_m ($3.6 \pm 0.3\,\mu M$) and k_{cat} ($0.55 \pm 0.04\,s^{-1}$) for cGMP hydrolysis by PDE5/6cd are similar to those reported for the PDE5 catalytic domain (PDE5cd), but they differ from the catalytic properties of PDE6 (K_m ~10–50 μM, k_{cat} ~2000–4000 s^{-1})(Supplementary Figure 1) (Arshavsky *et al*, 2002; Cote, 2004; Wang *et al*, 2006). Apparently, this is because most of the critical catalytic residues in PDE5/6cd are from PDE5. PDE5/6cd was potently and comparably inhibited by Pγ (K_i $1.5 \pm 0.2\,\mu M$) and $P\gamma_{63-87}$ (K_i $2.9 \pm 0.3\,\mu M$), whereas the inhibition by $P\gamma_{70-87}$ was somewhat less potent (K_i $12.1 \pm 1.8\,\mu M$) (Supplementary Figure 2A). In comparison, trypsin-activated PDE6 from bovine retina was inhibited by $P\gamma_{63-87}$ and $P\gamma_{70-87}$ with the K_i of 2.2 ± 0.3 and $3.7 \pm 0.4\,\mu M$, respectively (Supplementary Figure 2B). This suggests that PDE5/6cd retains most of the contacts between PDE6 and the Pγ C-terminus. To gain structural insights into the inhibitory interaction of the Pγ C-terminus with PDE6, we attempted to obtain crystals of unliganded PDE5/6cd and its complexes with Pγ, $P\gamma_{63-87}$, or $P\gamma_{70-87}$. In addition, crystallization screens were performed in the absence or presence of the catalytic-site inhibitors, sildenafil, and IBMX, to increase the number of potential candidates for crystal growth and explore potential drug–Pγ interactions at the catalytic site. Sildenafil and IBMX inhibited cGMP hydrolysis by PDE5/6cd with K_i values of 25 ± 2 nM and $8.5 \pm 0.6\,\mu M$, respectively (Supplementary Figure 1B and C). Diffracting crystals of the complexes of PDE5/6 bound with sildenafil or IBMX and $P\gamma_{70-87}$ were obtained and the structures were solved.

Structure of the sildenafil-bound PDE5/6cd

The crystal structure of PDE5/6cd in complex with sildenafil was solved at 2.9 Å to an R-factor of 22.3% and R-free of 27.5% (Table I). The final model contained four molecules per asymmetric unit, and residues 536–859 of molecules A and B, residues 535–859 of molecule C and residues 537–859 of molecule D could be modelled clearly in the electron density. Electron density was clearly visible for sildenafil in each of the four molecules. The Ramachandran plot showed 99.7% of the residues to be in the most favoured or allowed regions. Molecules A and C are almost indistinguishable, and likewise, molecules B and D are nearly identical (Supplementary Table I). Molecules A and B vary at two flexible regions defined earlier as the H-loop (residues 660–683) and M-loop (residues 788–811) (Huai *et al*, 2004; Wang *et al*, 2006) with the M-loop

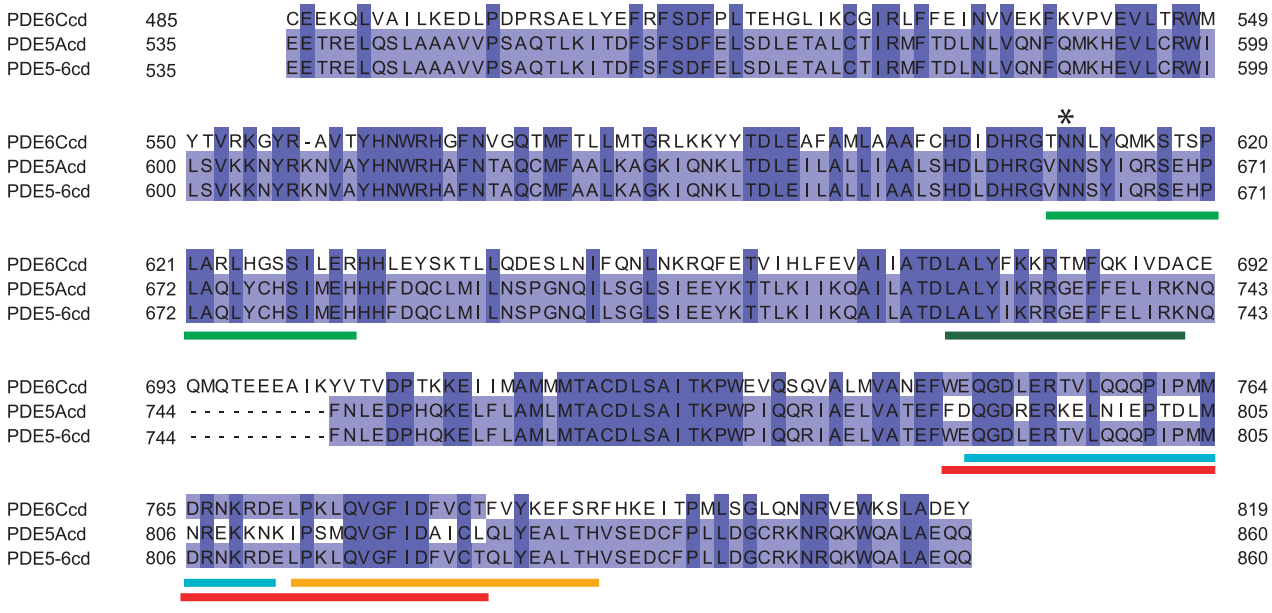

Figure 1 Sequence alignment of the catalytic domains of human PDE6C, PDE5A, and the chimaeric catalytic domain PDE5/6cd. The H- and M-loops are underlined with green and cyan lines, respectively. The α-helices 12 and 15 are underlined with dark green and orange lines, respectively. The PDE5cd H-loop/α-helix15 region that was replaced by the corresponding PDE6C sequence to generate PDE5/6cd is underlined with red line. Asterisk indicates PDE5/6cdAsn^{661}. Alignment was generated using ClustalW.

Table I Crystallographic data collection and refinement statistics

	PDE5/6cd–sildenafil crystal	PDE5/6cd–IBMX–Pγ_{70-87} crystal
Data collection statistics		
Space group	$P2_12_12_1$	$P2_12_12_1$
Cell dimensions	$a=75.7$	$a=47.3$
	$b=109.8$	$b=125.7$
	$c=199.7$	$c=153.9$
Resolution (Å)	29.8–2.9 (3.0–2.9)	40.4–3.0 (3.1–3.0)
R_{merge}	0.175 (0.563)	0.127 (0.328)
$I/\sigma I$	6.1 (2.0)	6.8 (2.9)
Completeness (%)	86.8 (76.9)	93.0 (87.0)
Redundancy	5.80 (5.05)	2.84 (2.39)
Refinement statistics		
Resolution (Å)	29.8–2.9	40.4–3.0
Number of reflections	31 941	17 894
R_{work}/R_{free} (%)	22.3/27.5	21.2/27.9
B-factor for protein (Å)	23.0	47.7
B-factor for ligand	54.5	58.0 (IBMX)/ 59.4 (Pγ_{70-87})
B-factor for ions	35.8	31.5
B-factor for water	16.0	22.7
r.m.s.d. bond length (Å)	0.015	0.007
r.m.s.d. bond angles (deg)	1.512	1.038
Number of protein atoms	10 570	5582
Number of ligand atoms	132	80
Number of ions	8	4
Number of water atoms	13	18
Ramachandran plot (% residues)		
Most favored	96.5	90.3
Additionally allowed	3.2	9.7
Disallowed	0.3	0

Values in parenthesis refer to the highest resolution shell.

being the most different (Supplementary Figure 3). The omit maps for the sildenafil molecules are shown in Supplementary Figure 4A. Interestingly, sildenafil adopts a different conformation within each molecule. The conformations of sildenafil bound to PDE5/6 molecules A and C are similar, as are the conformations of sildenafil bound to molecules B and D. The methylpiperazine group of sildenafil displays the most significant conformational change (Supplementary Figure 4B). Conformational variation of sildenafil has been recognized earlier in reported structures of sildenafil-bound PDE5cd (Wang *et al*, 2006). The conformational differences in the H- and M-loop regions and sildenafil between molecules A and B are likely caused by the packing in the asymmetric unit. Within the asymmetric unit, the four H-loops are in close proximity, as are the four M-loops (Supplementary Figure 5). However, in contrast to molecule B, the loop regions in molecule A seem to be minimally disturbed by packing (Supplementary Figure 6). Furthermore, the *B*-factors for the H- and M-loops are lower in molecule A compared with molecule B (Supplementary Figure 7A and B). Consequently, molecule A is used hereafter to describe the sildenafil-bound PDE5/6cd structure. The PDE5/6cd–sildenafil structure is compared with molecule A from the PDE5cd–sildenafil structure solved by Wang *et al*, as only in this structure both the H- and M-loops are fully present (Wang *et al*, 2006).

Except for the H- and M-loops, the overall structure of PDE5/6cd closely resembles the structure of PDE5cd in complex with sildenafil (Wang *et al*, 2006) (Supplementary

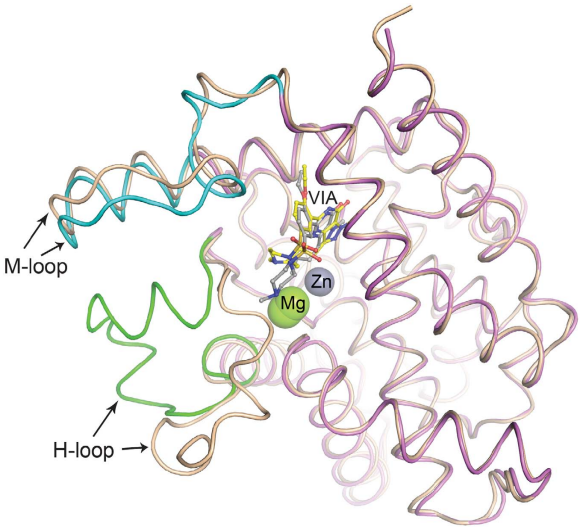

Figure 2 Superimposition of the structures of sildenafil-bound PDE5/6cd and PDE5cd. The H-loop (green) of PDE5/6cd (violet) is shifted to the left and the M-loop (cyan) is shifted down, bringing the two loops closer together compared with the loops of PDE5cd (wheat, PDB ID: 2H42). Grey—sildenafil (VIA) from PDE5/6cd structure; yellow—sildenafil from PDE5cd structure; light green spheres—magnesium ions (Mg); grey spheres—zinc ions (Zn).

Table I). The conformation of the H-loop in the PDE5/6cd–sildenafil structure is markedly different from that in the sildenafil-bound PDE5cd. Overlay of the sildenafil-bound PDE5/6cd and PDE5cd structures shows that the H-loop moves dramatically, up to 26.2 Å, towards the M-loop in the PDE5/6cd structure even though the H-loop sequences of both structures are the same (Figure 2). Reciprocally, the M-loop of the PDE5/6cd structure shifts up to 3.6 Å towards the bound sildenafil and H-loop. The conformations of the H- and M-loops in the PDE5/6cd structure are stabilized by an extensive interface between them. Residues Val^{660} and Tyr^{664} of the H-loop make hydrophobic interactions with M-loop residues Leu^{792}, Val^{796}, and Leu^{797} (Figure 3A). Additionally, polar residues Asn^{661} and Arg^{667} in the H-loop form contacts with residues Gln^{789}, Glu^{793}, and Gln^{799} in the M-loop, respectively. In the PDE5cd–sildenafil structure, there is only one molecule that has both loops present and the *B*-factors for both loops of that molecule are relatively high compared with the overall structure *B*-factor (Wang *et al*, 2006) (Supplementary Figure 7C). Only residues Asn^{661} and Ser^{663} in the H-loop, and Gly^{659} outside of the H-loop, come into contact with M-loop residues Gln^{789}, Arg^{792}, Leu^{804}, and Met^{805} in PDE5cd (Figure 3B). The ability of the H- and M-loops to establish a strong interface in PDE5/6cd seems to be determined by hydrophobic interactions involving the M-loop residues Leu^{792} and Val^{796}. PDE5cd instead contains Arg^{792} and Glu^{796}.

In addition to structural variations in the H- and M-loops, sildenafil assumes distinct conformations in complex with PDE5/6cd and PDE5cd. The pyrazolopyrimidinone and ethoxyphenyl groups of sildenafil occupy similar positions in the two structures. Most of the PDE5/6cd contact residues with the two groups are the same as in PDE5cd (Supplementary Figure 8). The differences are largely confined to residues that contact the methylpiperazine group of sildenafil. Specifically, PDE5/6cd residue Met^{804} (Leu^{804} in

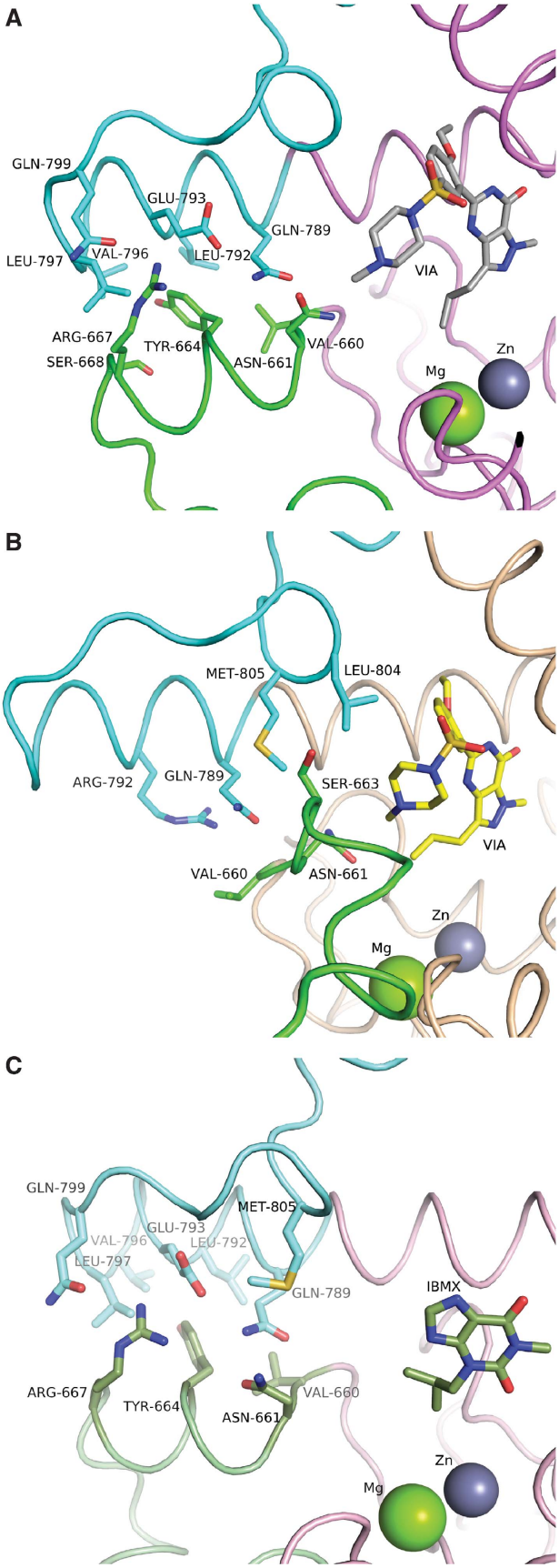

PDE5cd) extends towards the methylpiperazine group in the PDE5/6cd structure, which results in the methylpiperazine group to straighten more and interact with Phe^{823} (Ala^{823} in PDE5cd) (Supplementary Figure 8).

Structure of PDE5/6cd in complex with IBMX and Pγ_{70-87}

The crystal structure of PDE5/6cd in complex with IBMX and Pγ_{70-87} was solved at 3.0 Å with non-crystallographic symmetry (NCS) restraints to an R-factor of 21.2% and R-free of 27.9% (Table I). Each asymmetric unit contained two molecules of PDE5/6cd and two molecules of Pγ_{70-87} (Supplementary Figure 9A). PDE5/6cd residues 537–859 and 535–859 of molecules A and B, respectively, were modelled clearly in the electron density. Electron density was clear for residues 71–87 of the Pγ_{70-87} peptide, but not for Trp^{70}. Each PDE5/6cd molecule had one Pγ_{70-87} bound. The omit maps for Pγ_{70-87} are shown in Supplementary Figure 10. The Ramachandran plot showed all residues to be in the most favoured or allowed regions. PDE5/6cd molecules A and B are almost identical and Pγ_{70-87} molecules C and D are nearly indistinguishable (Supplementary Table I). Electron density was clearly visible for IBMX in the catalytic pocket of PDE5/6cd. IBMX bound to PDE5/6cd molecules A and B adopts a similar conformation except for the orientation of the isobutyl group. The xanthine ring stacks against Phe^{820} and binds to a pocket with the same residues as in the known structure of PDE5cd–IBMX (Supplementary Figure 11A and B). There were also three nonspecifically bound IBMX molecules between the asymmetric units (Supplementary Figure 11C). The omit maps for all IBMX molecules are shown in Supplementary Figure 11C.

Excluding the H- and M-loops, the structure of PDE5/6cd in complex with IBMX/Pγ_{70-87} is superimposable with the published structure of PDE5cd–IBMX (Huai *et al*, 2004) (Figure 4A; Supplementary Table I). The PDE5cd–IBMX structure is missing electron density for most of the M-loop residues and has higher *B*-factor values for the H-loop compared with PDE5/6cd bound with IBMX and Pγ_{70-87} (Supplementary Figure 12). The PDE5/6cd H-loop adopts a different conformation than the H-loop of PDE5cd–IBMX with a divergence up to a 10.2 Å (Figure 4A). Remarkably, conformations of the H- and M-loops are similar in the structures of PDE5/6cd complexed with IBMX–Pγ_{70-87} and sildenafil (Figure 4B). The two structures align with an r.m.s.d of 0.49 over 323 Cα atoms (Supplementary Table I). Both structures have good *B*-factor values for both of the loop regions compared with the overall structure *B*-factors (Supplementary Figures 7 and 12). The H–M-loop interface in the PDE5/6cd—IBMX–Pγ_{70-87} complex involves the same residues as the H–M-loop interface in the sildenafil-bound PDE5/6cd (Figure 3C). The side chains of the residues within

Figure 3 H- and M-loop interactions in PDE5/6cd and PDE5cd. Close-up view of the interactions between the H- and M-loops of the PDE5/6cd (**A**) and PDE5cd (**B**) complexes with sildenafil. Colours as listed in Figure 2. (**C**). Interactions between the H-loop (pale green) and the M-loop (pale cyan) of the PDE5/6cd (light pink) complex with IBMX (dark green) and Pγ_{70-87}. Pγ_{71-87} is omitted so as not to block the view of the interactions between the loops.

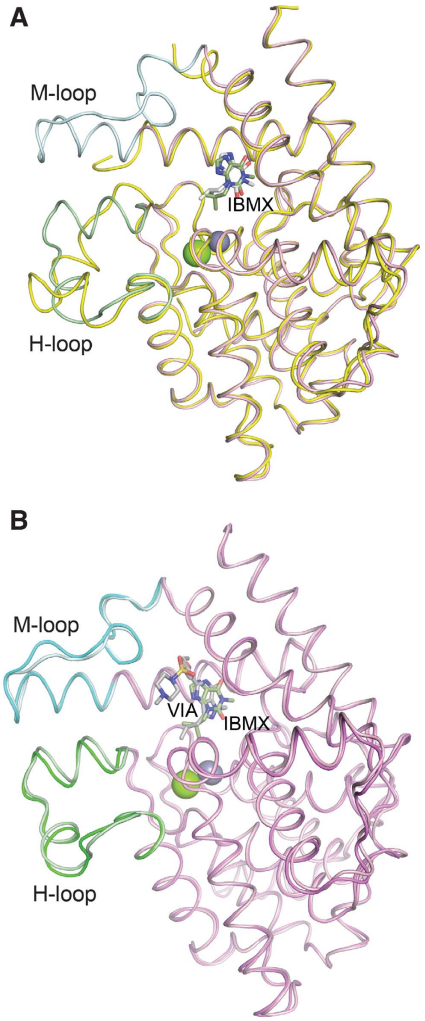

Figure 4 (**A**) Superimposition of IBMX-bound structures of PDE5/6cd and PDE5cd. The PDE5cd structure (yellow, PDB ID: 1RKP) with bound IBMX (white) is missing most of the M-loop residues. Light pink—PDE5/6cd; pale green—H-loop of PDE5/6cd; pale cyan—M-loop of PDE5/6cd; dark green—IBMX bound to PDE5/6cd. (**B**). Superposition of the sildenafil- and IBMX–Pγ_{70-87}-bound structures of PDE5/6cd. Colours same as listed in Figures 2 and 4 (A).

the H- and M-loops are relatively close in conformation in the two PDE5/6cd structures (Supplementary Figure 13).

Conformation of Pγ_{70-87} and its interface with PDE5/6cd

Residues 76–83 of Pγ_{70-87} bound to PDE5/6-IBMX form an α-helix and residues 84–87 form a cap near the active site (Figure 5A). The conformation of residues 71–74 may be affected by the crystal packing. Residues 71–74 of Pγ come within close proximity with the neighbouring asymmetric unit, although there are no meaningful interactions between them (Supplementary Figure 9B and C). The interactions between Pγ_{70-87} and PDE5/6cd involve residues from the H- and M-loops and α-helixes 12 and 15, and are a combination of hydrophobic, electrostatic, and Van der Waals interactions (Figure 5B–D). The Pγ peptide blocks the active site of PDE5/6cd by completely filling the opening of the catalytic cavity (Figure 6). PDE5/6cd α-helix 12 residues Leu^{725}, Ala^{726}, and Ile^{729} form interactions with Pγ residues Phe^{73}, Leu^{81}, and Ile^{86} (Figure 5B). H-loop residues Asn^{661}, Asn^{662}, and Ser^{663} interact with the Pγ C-terminal cap residues Gly^{85} and Ile^{87}, whereas Gln^{666}, His^{678}, and Ser^{679} make contacts with the Pγ residue Glu^{71} (Figure 5C). M-loop residues Ile^{802} and Met^{804} interact with Pγ residues Ala^{82}, Gln^{83}, Tyr^{84}, and Gly^{85}, and α-helix 15 residues Phe^{820}, Phe^{823}, and Val^{824} make contacts with Glu^{80}, Leu^{81}, Gln^{83}, and Tyr^{84} of Pγ (Figure 5D). PDE5/6cd Ile^{802}, Pro^{803}, Met^{804}, and Leu^{816} form a barrier, thus terminating the α-helix of Pγ and inducing the C-terminal cap (Figure 5D). Pγ_{70-87} conformation is also stabilized by intramolecular interactions involving hydrophobic residues Phe^{73}, Leu^{78}, Leu^{81}, and Ile^{87}.

Mutational analysis of PDE5/6cdAsn^{661} implicated in the atrd3 mouse model of retinal degeneration

The PDE5/6cd–IBMX–Pγ_{70-87} structure is consistent with the role of the PDE6 M-loop/α-helix 15 region and two key residues, Met^{804} and Phe^{823}, in the inhibitory interaction with Pγ (Granovsky and Artemyev, 2000, 2001a). However, the structure also indicates earlier unrecognized roles of the H-loop and α-helix 12 in the PDE6–Pγ interface. Residue Asn^{661} from the H-loop is of particular interest because it contacts the Pγ backbone at Gly^{85} and is a part of the H–M-loop interface that is essential for Pγ binding. Furthermore, the Asn→Ser mutation of the corresponding residue Asn^{605} in PDE6B causes retinal degeneration in *atrd3* mice (Hart *et al*, 2005). Two mutant PDE5/6cd proteins, Asn^{661}Ser and Asn^{661}Ala, have been generated to probe the role of Asn^{661} in Pγ binding and the mechanism of *atrd3*. The enzymatic properties of the PDE5/6cdAsn^{661}Ser mutant were similar to those of PDE5/6cd (Supplementary Figure 1). The analysis of inhibition of the PDE5/6cdAsn^{661}Ser mutant by Pγ indicated a ~three-fold reduction in its affinity for the PDE6-inhibitory subunit (Figure 7). The Asn^{661}Ala substitution moderately increased the K_m value for cGMP hydrolysis (Supplementary Figure 1), but it markedly decreased the potency of PDE5/6cd inhibition by Pγ (Figure 7).

The Pγ contact residues within α-helix 12 of PDE5/6cd are also involved in the intramolecular interactions essential for the integrity of the catalytic site. To examine the role of α-helix 12 in the Pγ-binding interface, Ile^{729} was selected for mutagenesis because it is the farthest from the catalytic pocket. Even so, the Ile^{729}Ala mutation markedly reduced the activity of PDE5/6cd, precluding evaluation of the mutation effect on the inhibition by Pγ.

Discussion

The inhibition of PDE6 by the small protein modulator Pγ is unique among the superfamily of PDEs and is one of the central interactions in the visual transduction cascade. The atomic structure of the key inhibitory Pγ fragment Pγ_{70-87} bound to a chimaeric PDE5/6 catalytic domain shows the molecular determinants for the selectivity of PDE6–Pγ interaction and the mechanism of PDE6 inhibition by Pγ. The structure also has important implications for the mechanism of PDE6 activation by transducin.

The H–M loop interface in PDE5/6cd is critical for the selective interaction with the Pγ C-terminus

With the exception of two variable H- and M-loops, the core structures of PDE catalytic domains are very similar. Positions and conformations of these loops in PDE5cd are highly

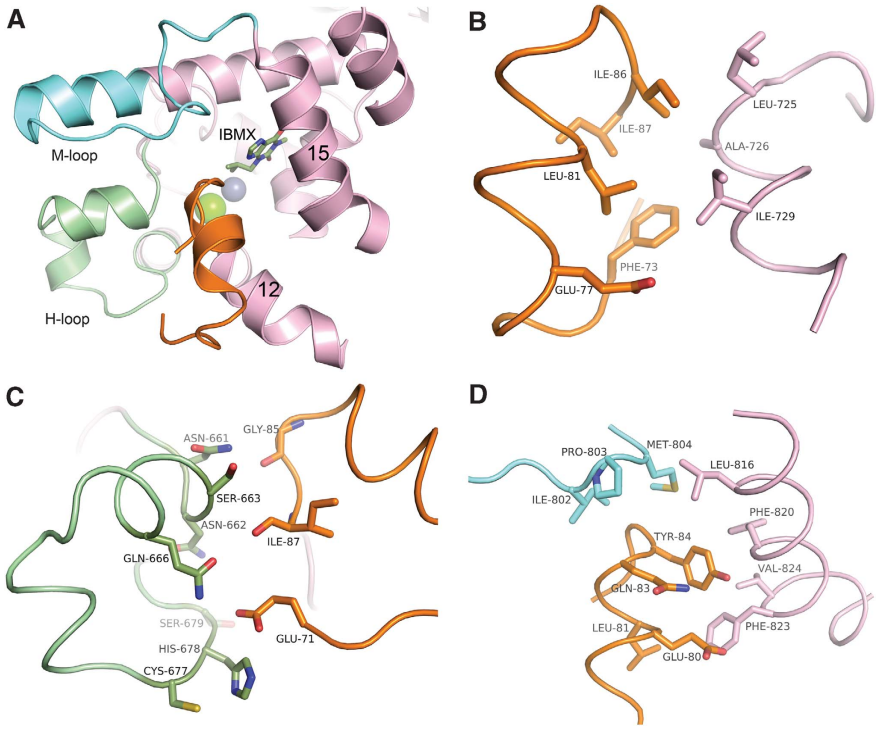

Figure 5 $P\gamma_{71-87}$ interactions with PDE5/6cd. (**A**) Ribbon representation of $P\gamma_{71-87}$ (orange) bound to PDE5/6cd. The C-terminal residues of Pγ are close to IBMX, but they do not form an interaction. α-helices 12 and 15 are labelled 12 and 15, respectively. (**B**) Interactions between $P\gamma_{71-87}$ and helix 12 of PDE5/6cd. (**C**) Interactions between PDE5/6cd H-loop and $P\gamma_{71-87}$. (**D**) Interactions between $P\gamma_{71-87}$ and PDE5/6cd M-loop and helix 15. Interacting residues are labelled accordingly. Colours same as listed in Figure 4 A.

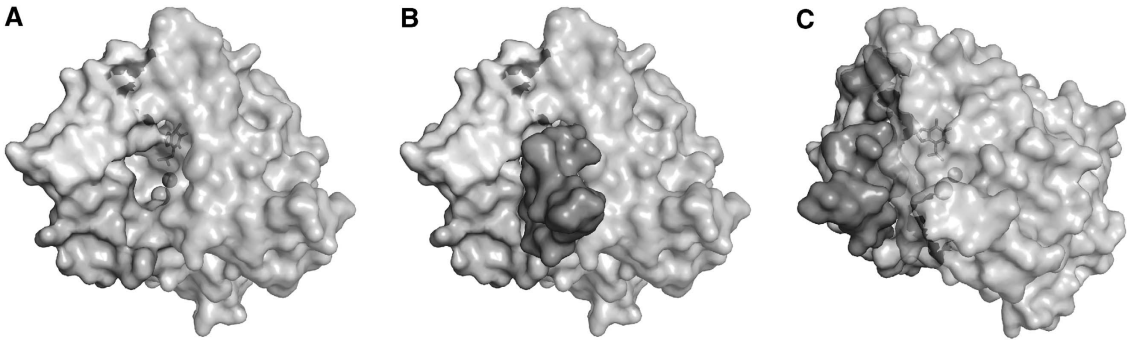

Figure 6 $P\gamma_{71-87}$ completely blocks the active site of PDE5/6cd. Surface representation of the active-site pocket without (**A**) and with (**B**) $P\gamma_{71-87}$ bound. (**C**) A 50° rotation about the *x* axis with $P\gamma_{71-87}$ bound to PDE5/6cd.

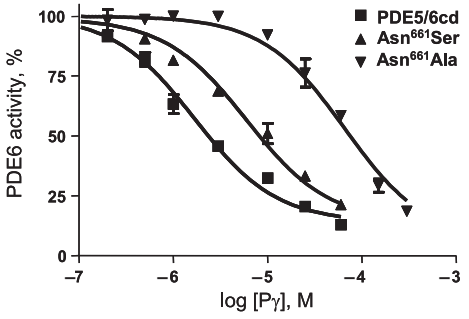

Figure 7 Inhibition of PDE5/6cd and its $Asn^{661}Ser$ and $Asn^{661}Ala$ mutants by Pγ. The activity of PDE5/6cd and its mutants was measured in the presence of 0.5 μM cGMP and increasing concentrations of Pγ. Results from one of three similar experiments are shown. The calculated K_i values for PDE5/6cd, the $Asn^{661}Ser$, and $Asn^{661}Ala$ mutants were 1.5 ± 0.2, 4.6 ± 0.4, and 62 ± 8 μM (mean ± s.e.), respectively.

sensitive to the nature of ligand bound to the active site (Sung *et al*, 2003; Huai *et al*, 2004; Wang *et al*, 2006). In contrast, the structures of PDE5/6cd–sildenafil and PDE5/6cd—IBMX–$P\gamma_{70-87}$ showed surprisingly comparable conformations of the H- and M-loops, which are stabilized by extensive inter-loop interactions. Two PDE6-specific residues from the M-loop, Leu^{792} and Val^{796}, are intimately involved in the H–M loop interface that distinguishes the structure of PDE5/6cd from structures of PDE5cd and other PDE catalytic domains. Thus, the H–M loop interface is an intrinsic attribute of PDE5/6cd and, in all probability, PDE6. The propensity of PDE5/6cd to form this interface might be further augmented by binding of sildenafil or IBMX/$P\gamma_{70-87}$.

The structure of the PDE5/6cd—IBMX–Pγ70-87 complex shows that the H–M loop interface is an essential component in the formation of the Pγ-binding site. The Pγ-binding

surface is comprised of residues from four structural elements: the M-loop and α-helix 15, and the newly recognized H-loop and α-helix 12. The H–M loop interface favourably positions the H-loop residues Asn^{661}, Asn^{662} and Ser^{663} (Leu in PDE6), and the PDE6-specific M-loop residues Ile^{802} and Met^{804} for the interactions with the Pγ C-terminus. Apparently, the absence of the comparable H–M loop interface in PDE5 is one of the main reasons for the failure of Pγ to inhibit this enzyme. Another major determinant for the selectivity of PDE6 inhibition by Pγ is Phe^{823} (Ala in PDE5) in α-helix 15 (Granovsky and Artemyev, 2001a). The side chain of Phe^{823} makes multiple contacts with the side chains of Pγ Glu^{80}, Leu^{81}, Tyr^{84} and Ile^{86}, making it indispensable for binding the Pγ C-terminus. Thus, three of the four Pγ-binding elements, H-loop, M-loop, and α-helix 15, are essential to the selectivity of the interaction. The fourth Pγ-binding segment localized at the start of α-helix 12 is largely conserved in PDE5 and PDE6 and assumes similar conformations in the structures of PDE5cd and PDE5/6cd.

The structure of the PDE-bound Pγ C-terminus illuminates the PDE6 inhibition mechanism and suggests Pγ conformational change on activation by transducin

A recent NMR study of free Pγ has concluded that it is an intrinsically disordered protein, which nonetheless contains functionally significant transient secondary and tertiary structure (Song *et al*, 2008). Furthermore, the analysis suggested that residues 68–84 in free Pγ are ~50% helical. In the structure of the PDE5/6cd-bound $P\gamma_{70-87}$, residues 76–83 form an α-helix with a cap involving residues 84–87. Therefore, the α-helix 76–83 may represent a preconfigured conformation in the free Pγ that favours its binding to PDE6. The C-terminal cap 84–87 then fits snugly into the opening of the catalytic pocket and occludes access of cGMP to the active site (Figure 6). The role of many of the PDE6 contact residues of Pγ (Figure 5) in PDE6 inhibition is consistent with previous biochemical studies (Skiba *et al*, 1992; Granovsky and Artemyev, 2001b). Comparison of the PDE5/6cd-bound conformation of the Pγ C-terminus with that when bound to the transition–state complex of $G\alpha_t$ (Slep *et al*, 2001) provides important insights into the mechanism of PDE6 activation by transducin. In the PDE5/6- and $G\alpha_t$-bound states, the Pγ C-terminal residues 78–87 adopt similar conformations featuring α-helices and C-terminal caps. As a consequence, the 10 C-terminal Cα atoms of Pγ in the two complexes are superimposable with r.m.s.d of 0.617. However, transducin binding shortens the C-terminal α-helix of Pγ from residues 76–83 to 78–83 and alters the conformation of residues 71–77. This suggests a mechanism whereby $G\alpha_t$GTP interaction with the PDE6-bound Pγ induces a conformational change encompassing Pγ residues 71–77 and results in a hinge-like rigid-body movement of Pγ-78–87 away from the PDE6 catalytic pocket. Two transducin-contact residues of Pγ, Trp^{70}, and Leu^{76} were shown earlier to be unimportant for PDE6 inhibition but critical for PDE6 activation by transducin (Slepak *et al*, 1995; Tsang *et al*, 1998; Slep *et al*, 2001; Granovsky and Artemyev, 2001b). Indeed, the structure shows that PγLeu^{76} points away from PDE5/6cd and is readily accessible for binding to $G\alpha_t$. Accordingly, we propose that Trp^{70} and Leu^{76} serve as anchors for the initial docking of $G\alpha_t$GTP that leads to the activational displacement of the Pγ C-terminus from PDE6. Subsequently, $G\alpha_t$ engages additional Pγ residues, such as Phe^{73}, Leu^{81}, and Ile^{87}, that are relieved from the interface with PDE6 (Supplementary Figure 14).

Disruption of the PDE6–Pγ interaction by a mutation causing atypical retinal degeneration in mice

Three novel mutations in the *Pde6b* gene were identified earlier that lead to a relatively slow onset of retinal degeneration in mice. The mutant lines were termed *atrd1–atrd3* for atypical retinal degeneration (Thaung *et al*, 2002; Hart *et al*, 2005). The *atrd3* allele was originally reported to carry the missense mutation Asn^{606}Ser (Hart *et al*, 2005). However, our sequencing of DNA obtained from *atrd3* mice indicated an Asn^{605}Ser mutation, which is in agreement with the current annotation of the mutant allele at the Mouse Genome Informatics database (ID: MGI:2178316). The position corresponding to Asn^{605} in mouse PDE6B is not absolutely conserved among PDEs. PDE4 contains a Ser residue at this position, which is analogous to the Asn→Ser substitution in *atrd3* mice. The lack of absolute conservation and the slow progression of retinal degeneration in *atrd3* mice suggest that this mutation leads to change rather than loss of PDE6 function. PDE5/6cdAsn^{661}, a counterpart of PDE6BAsn^{605}, is a key H-loop residue interacting with the M-loop Gln^{789} and PγGly^{85} (Supplementary Figure 15A). The Asn^{661}Ser mutation moderately reduced the ability of Pγ to inhibit PDE5/6cd. This effect agrees with the modelling of the Asn^{661}Ser substitution into the PDE5/6cd—IBMX–$P\gamma_{70-87}$ structure. The side chain of Ser is able to maintain either a hydrogen bond with PγGly^{85} or with the M-loop Gln^{789}, but not both contacts simultaneously (Supplementary Figure 15B and C). Analysis of the Asn^{661}Ala mutation showed a much more severe impairment of the inhibition by Pγ (Figure 7). The Ala residue is predicted to loose both of the contacts with PγGly^{85} and M-loop Gln^{789} (Supplementary Figure 15D). These results confirm the role of the H–M loop interface in the PDE5/6cd–Pγ interaction and suggest that it is disrupted in *atrd3* mice.

Interplay of the Pγ C-terminus and sildenafil at the catalytic site of PDE6

PDE5 inhibitors sildenafil (Viagra) and vardenafil (Levitra) are widely used in the treatment of erectile dysfunction. However, these drugs are also potent inhibitors of PDE6 thereby causing vision impairments in some patients. The adverse effects include a blue tinge to vision, increased brightness of lights, blurry vision, and difficulty in discriminating objects (Laties and Sharlip, 2006). Recent reports indicate that sildenafil lengthens the response time of both rods and cones significantly compared with a placebo group, thus possibly impairing the ability of the eye to adapt to light and regulate its sensitivity (Stockman *et al*, 2006, 2007). At the biochemical level, in contrast to a potent inhibition of activated PDE6, sildenafil is a poor inhibitor of holoPDE6. Consistent with the proposed competition at the catalytic site, low concentrations of sildenafil cause paradoxical activation of holoPDE6 (Zhang *et al*, 2005). Potential interactions of sildenafil and Pγ at the catalytic site of PDE6 are thought to be critical to understanding the mechanism of sildenafil's effects on vision (Zhang *et al*, 2005). The sildenafil- and $P\gamma_{70-87}$-bound structures of PDE5/6cd provide rationale for the observed effects of sildenafil on PDE6.

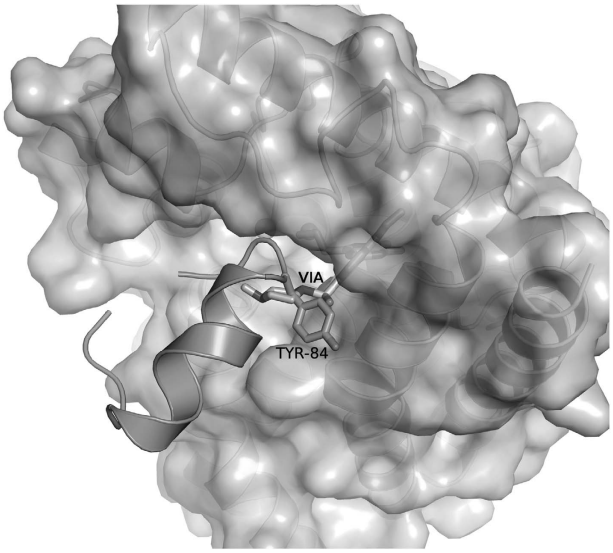

Figure 8 Sildenafil clashes with PγTyr^{84}. In the superimposed model of the sildenafil-bound PDE5/6cd structure and the IBMX/Pγ$_{70-87}$-bound PDE5/6cd structure, Pγ$_{70-87}$ clashes with sildenafil (VIA). The IBMX/Pγ$_{70-87}$-bound PDE5/6cd structure is shown in surface representation. PγTyr^{84} is shown as sticks.

Several sildenafil-binding residues of PDE5/6cd such as Leu^{725}, Met^{804}, Phe^{820} and Phe^{823} also serve as Pγ contacts. The overlay of the sildenafil- and Pγ$_{70-87}$-bound structures of PDE5/6cd shows a wide clash between the methylpiperazine group and PγTyr^{84} (Figure 8). From the PDE5/6cd structures, the interactions of the drug and Pγ with the catalytic domain seem to be mutually exclusive. Yet, we found that Pγ$_{63-87}$ co-migrates with the PDE5/6cd–sildenafil complex during native gel electrophoresis (Supplementary Figure 16). As the methylpiperazine group of sildenafil was shown to adopt multiple conformations in complexes with PDE5/6cd or PDE5cd, it may take on a conformation that allows for stacking against the PγTyr^{84}. Still, the Pγ interaction with PDE5/6cd is predicted to be weakened when sildenafil is bound to the catalytic pocket. Further, an alteration of the Pγ C-terminus conformation caused by sildenafil may interfere with the ability of transducin to bind and activate PDE6. Our structural studies may aid in the design of selective PDE5 inhibitors lacking side effects on vision.

Materials and methods

Expression, purification, mutagenesis and characterization of PDE5/6cd

The PDE5/6cd chimaera based on sequences of human PDE5 and PDE6C is different from the bovine PDE5/PDE6 chimaera C6 (Muradov *et al*, 2006) at five amino acid residues. The DNA sequence corresponding to human PDE5 residues 535–786 was amplified with RT–PCR using total RNA from HEK293 cells as a template. This DNA fragment was replaced into the C6 chimaera vector using Nde I and Bgl II sites, thus allowing the changing of four out of five different residues. The remaining different amino acid residue was replaced using the QuikChange Mutagenesis protocol (Stratagene). The PDE5/6cd plasmid was transformed into BL21-codon plus competent cells (Stratagene). Expression and purification of the His6-tagged PDE5/6cd over His-bind resin (Novagen) was performed as described earlier (Muradov *et al*, 2006). The eluted protein was diluted two-fold with buffer A (20 mM Tris–HCl, pH 7.5, containing 50 mM NaCl and 1 mM β-mercaptoethanol). Thrombin (final concentration 0.4 units/μl; Sigma Aldrich) and $MgSO_4$ (10 mM) were added to the protein followed by incubation for 16 h at 4°C. The thrombin-cleaved PDE5/6cd was passed over $NiSO_4$-charged His-bind resin for a second time and the flow-through fraction was collected and concentrated to a final volume of ~5 ml using Amicon Ultra (30 000 MWCO; Millipore) filters. The concentrated protein was centrifuged (13 000 *g*, 10 min, 4°C) and loaded onto Benzamidine sepharose (HiTrap Benzamidine FF; GE Healthcare) using buffer A at 1 ml/min. Protein was eluted for 24 min with buffer A, and then for another 24 min with buffer A plus 500 mM NaCl. All fractions containing protein were combined and concentrated to a final volume of ~5 ml using Amicon Ultra (30 000 MWCO) filters and loaded onto Superdex 75 sepharose (GE Healthcare) using buffer A at 1 ml/min. Fractions containing PDE5/6cd were combined and concentrated to a desired concentration (15–30 mg/ml). The purity of the protein was assessed by SDS–PAGE in 12.5% gels and Coomassie Blue staining. The PDE5/6cd protein concentration was calculated by measuring the A_{280} using a NanoDrop spectrophotometer (Thermo Scientific) and $\varepsilon = 38\,234$ cm/M. The monodispersity of concentrated PDE5/6cd was measured by dynamic light scattering (Protein Solutions/Wyatt Technology) at 4°C after ultracentrifugation (45 000 *g*, 20 min, 4°C). Preparations of PDE5/6cd with the polydispersity under 30% were stored at −80°C in 10 μl aliquots for later use. Typically, 1.5 l of cell pellets yielded ~5 mg of >95% pure PDE5/6cd.

The PDE5/6cd mutants Asn^{661}Ser, Asn^{661}Ala, and Ile^{729}Ala were constructed according to the Quik Change Mutagenesis protocol (Stratagene). The sequences of all constructs were verified by automated DNA sequencing at the University of Iowa DNA Core Facility. The PDE5/6cd mutants were purified similarly to PDE5/6cd, except the His-tag cleavage with thrombin and chromatography over Benzamidine sepharose were omitted. Control experiments showed no differences in properties of PDE5/6cd before or after removing the His6-tag with thrombin. PDE5/6cd activity was measured using 0.5 μM [^{3}H]cGMP and 0.5–5 nM PDE5/6cd according to published protocols (Muradov *et al*, 2006). Purified trypsin-activated bovine rod PDE6 was obtained as described (Artemyev *et al*, 1996). Bovine PDE6 activity was measured using 5 μM [^{3}H]cGMP and 2 pM PDE6. The K_m and k_{cat} for cGMP hydrolysis and the K_i values for Pγ$_{63-87}$ and Pγ$_{70-87}$ were determined as described (Muradov *et al*, 2006). The K_i values for PDE5/6cd inhibition by sildenafil and IBMX were calculated from the corresponding IC_{50} values using equation $K_i = IC_{50}/(1 \pm [cGMP]/K_m)$ (Cheng and Prusoff, 1973) and the PDE5/6cd K_m value of 3.6 μM cGMP. The K_m, K_i, and k_{cat} values are expressed as mean ± s.e. for three separate experiments. Analysis of co-migration of unliganded, IBMX- or sildenafil-bound PDE5/6cd with Pγ$_{63-87}$ using native gel electrophoresis and western blotting with anti-Pγ$_{63-87}$ antibodies was performed as described earlier (Muradov *et al*, 2006).

Crystallization and data collection

Sildenafil (Pfizer) was purified from tablets by reverse-phase chromatography using a Proteins C-4 column (Rainin), lyophilized, dissolved in H_2O, and stored in aliquots at −80°C before use. The concentration of sildenafil was determined by measuring the A_{289} using a NanoDrop spectrophotometer and $\varepsilon = 13\,800$ cm/M. PDE5/6cd and sildenafil were combined at 1:1.5 molar ratio and the protein–drug complex was ultracentrifuged at 45 000 *g* for 20 min at 4°C. The plate-shaped crystals of PDE5/6cd bound with sildenafil were grown by hanging drop vapour diffusion at 4°C against well buffer containing 100 mM Tris (pH 8.5), 200 mM $MgSO_4$, 12% PEG-3350, and 2.5% ethanol. The crystals appeared after 3 weeks. Diffraction data for the PDE5/6cd–sildenafil crystal were collected at the Industrial Macromolecular Crystallography beamline at the Advanced Photon Source (Argonne National Laboratory, Chicago, IL). The crystal belonged to the spacegroup $P2_12_12_1$ and diffracted to a resolution of 2.9 Å.

PDE5/6cd was mixed with IBMX (Sigma Aldrich) at 1:1.5 molar ratio and the complex was ultracentrifuged at 45 000 *g* for 20 min at 4°C. The Pγ peptide Pγ$_{70-87}$ was custom made by Sigma-Genosys and purified by reverse-phase HPLC. The PDE5/6cd–IBMX complex and Pγ$_{70-87}$ were combined at a 1:1.25 molar ratio, incubated for 1 h on ice, and ultracentrifuged at 45 000 *g* for 20 min at 4°C. The thin rod shaped crystals of PDE5/6cd bound with IBMX and Pγ$_{70-87}$ grew within 3 days at 20°C against buffer containing 100 mM HEPES (pH 8.0), 1 M sodium citrate (pH 8.0), and 2.5% ethanol. Data for

the crystal were collected remotely from the University of Iowa Protein Crystallography Facility using the 4.2.2 beamline at the Advanced Light Source (Berkeley, CA). The crystal belonged to the $P2_12_12_1$ spacegroup and diffracted to 3.0 Å.

Structure determination

Data for PDE5/6cd bound to sildenafil were processed using d*TREK (Pflugrath, 1999). Phaser was used to solve the structure by molecular replacement using the PDE5cd structure bound to sildenafil (PDB entry: 2H42) as a template (Read, 2001; Wang *et al*, 2006). Sildenafil and the metals were removed from the template before use in molecular replacement. Refinement was performed using the program Refmac5 of the CCP4-5.0.2 suite of programs (Collaborative Computational Project Number 4, 1994; Murshudov *et al*, 1997). Coot was used for molecular visualization and model building (Emsley and Cowtan, 2004). NCS between the four molecules was used in the refinement with tight restraints between chains A and C and between chains B and D. The metals (Mg and Zn) and Sildenafil were modelled into clearly visible electron densities. Regions of the H- and M-loops were deleted and incrementally rebuilt into the electron density. Waters were finally added to the structure using Coot, followed by manual editing. The final coordinates have been deposited to the Protein Data Bank (PDB ID: 3JWQ).

Diffraction data for PDE5/6cd bound to IBMX and $P\gamma_{70-87}$ were also processed using d*TREK (Pflugrath, 1999). Phaser was again used to solve the structure by molecular replacement using the PDE5/6cd structure bound with sildenafil as a template with the drug and the metals removed (Read, 2001). As before, refinement was performed using Refmac5 and model building using Coot (Collaborative Computational Project Number 4, 1994; Murshudov *et al*, 1997; Emsley and Cowtan, 2004). Tight NCS restraints were used between the two PDE5/6cd molecules in the asymmetric unit during refinement. Mg, Zn, and IBMX could easily be modelled in the electron density but the $P\gamma_{70-87}$ peptide had to be incrementally built in Coot, followed by refinement in Refmac5. Finally, waters were added to the structure as before. The final coordinates have been deposited to the Protein Data Bank (PDB ID: 3JWR).

Supplementary data

Supplementary data are available at *The EMBO Journal* Online (http://www.embojournal.org).

Acknowledgements

We thank Alexey Surguchev for setting up crystallization trays for the PDE5/6cd–sildenafil complex and Jay Nix and Eric N Brown for assistance with the diffraction data collection. This work was supported by the National Institutes of Health grant EY-10843 to NOA and the American Heart Association pre-doctoral fellowship 0815399G to BB. Use of the IMCA-CAT beamline 17-ID at the Advanced Photon Source was supported by the companies of the Industrial Macromolecular Crystallography Association through a contract with the Center for Advanced Radiation Sources at the University of Chicago. Use of the Advanced Photon Source was supported by the US Department of Energy, Office of Science, Office of Basic Energy Sciences, under Contract No W-31-109-Eng-38.

Conflict of interest

The authors declare that they have no conflict of interest.

References

Arshavsky VY, Lamb TD, Pugh Jr EN (2002) G proteins and phototransduction. *Annu Rev Physiol* **264:** 153–187

Artemyev NO, Hamm HE (1992) Two-site high-affinity interaction between inhibitory and catalytic subunuts of rod cyclic GMP phosphodiesterase. *Biochem J* **283:** 273–279

Artemyev NO, Natochin M, Busman M, Schey KL, Hamm HE (1996) Mechanism of photoreceptor PDE inhibition by its γ-subunits. *Proc Natl Acad Sci USA* **93:** 5407–5412

Card GL, England BP, Suzuki Y, Fong D, Powell B, Lee B, Luu C, Tabrizizad M, Gillette S, Ibrahim PN, Artis DR, Bollag G, Milburn MV, Kim SH, Schlessinger J, Zhang KY (2004) Structural basis for the activity of drugs that inhibit phosphodiesterases. *Structure* **12:** 2233–2247

Cheng Y, Prusoff WH (1973) Relationship between the inhibition constant (K_i) and the concentration of inhibitor which causes 50 per cent inhibition (IC_{50}) of an enzymatic reaction. *Biochem Pharmacol* **22:** 3099–3108

Collaborative Computational Project Number 4 (1994) The CCP4 suite: programs for protein crystallography. *Acta Crystallogr Section D Biol Crystallogr* **50:** 760–763

Conti M, Beavo J (2007) Biochemistry and physiology of cyclic nucleotide phosphodiesterases: essential components in cyclic nucleotide signaling. *Annu Rev Biochem* **76:** 481–511

Cote RH (2004) Characteristics of photoreceptor PDE (PDE6): similarities and differences to PDE5. *Int J Impot Res* **16**(Suppl 1)**:** S28–S33

Emsley P, Cowtan K (2004) Coot: model-building tools for molecular graphics. *Acta Crystallogr Section D Biol Crystallogr* **60:** 2126–2132

Francis SH, Corbin JD, Bischoff E (2009) Cyclic GMP-hydrolyzing phosphodiesterases. *Handb Exp Pharmacol* **191:** 367–408

Fu Y, Yau KW (2007) Phototransduction in mouse rods and cones. *Pflugers Arch* **454:** 805–819

Granovsky AE, Natochin M, Artemyev NO (1997) The γ-subunit of rod cGMP-phosphodiesterase blocks the enzyme catalytic site. *J Biol Chem* **272:** 11686–11689

Granovsky AE, Natochin M, McEntaffer RL, Haik TL, Francis SH, Corbin JD, Artemyev NO (1998) Probing domain functions of chimeric PDE6α′/PDE5 cGMP-phosphodiesterase. *J Biol Chem* **273:** 24485–24490

Granovsky AE, Artemyev NO (2000) Identification of the γ-subunit interacting residues on photoreceptor cGMP phosphodiesterase, PDE6α′. *J Biol Chem* **275:** 41258–41262

Granovsky AE, Artemyev NO (2001a) Partial reconstitution of photoreceptor cGMP phosphodiesterase characteristics in cGMP phosphodiesterase-5. *J Biol Chem* **276:** 21698–21703

Granovsky AE, Artemyev NO (2001b) A conformational switch in the inhibitory γ-subunit of PDE6 upon the enzyme activation by transducin. *Biochemistry* **40:** 13209–13215

Guo LW, Muradov H, Hajipour AR, Sievert MK, Artemyev NO, Ruoho AE (2006) The inhibitory γ subunit of the rod cGMP phosphodiesterase binds the catalytic subunits in an extended linear structure. *J Biol Chem* **281:** 15412–15422

Hart AW, McKie L, Morgan JE, Gautier P, West K, Jackson IJ, Cross SH (2005) Genotype-phenotype correlation of mouse Pde6b mutations. *Invest Ophthalmol Vis Sci* **46:** 3443–3450

Huai Q, Liu Y, Francis SH, Corbin JD, Ke H (2004) Crystal structures of phosphodiesterases 4 and 5 in complex with inhibitor 3-isobutyl-1-methylxanthine suggest a conformation determinant of inhibitor selectivity. *J Biol Chem* **279:** 13095–13101

Lamb TD, Pugh Jr EN (2006) Phototransduction, dark adaptation, and rhodopsin regeneration the proctor lecture. *Invest Ophthalmol Vis Sci* **47:** 5137–5152

Laties A, Sharlip I (2006) Ocular safety in patients using sildenafil citrate therapy for erectile dysfunction. *J Sex Med* **3:** 12–27

Liu X, Bulgakov OV, Wen XH, Woodruff ML, Pawlyk B, Yang J, Fain GL, Sandberg MA, Makino CL, Li T (2004) AIPL1, the protein that is defective in Leber congenital amaurosis, is essential for the biosynthesis of retinal rod cGMP phosphodiesterase. *Proc Natl Acad Sci USA* **101:** 13903–13908

Mou H, Cote RH (2001) The catalytic and GAF domains of the rod cGMP phosphodiesterase (PDE6) heterodimer are regulated by distinct regions of its inhibitory γ subunit. *J Biol Chem* **276:** 27527–27534

Muradov KG, Granovsky AE, Schey KL, Artemyev NO (2001) Direct interaction of the inhibitory γ-subunit of rod cGMP phosphodiesterase (PDE6) with the PDE6 GAFa domains. *Biochemistry* **41:** 3884–3890

Muradov H, Boyd KK, Artemyev NO (2006) Analysis of PDE6 function using chimeric PDE5/6 catalytic domains. *Vision Res* **46:** 860–868

Murshudov GN, Vagin AA, Dodson EJ (1997) Refinement of macromolecular structures by the maximum-likelihood method. *Acta Crystallogr Section D Biol Crystallogr* **53:** 240–255

Pflugrath JW. (1999) The finer things in X-ray diffraction data collection. *Acta Crystallogr Section D Biol Crystallogr* **55:** 1718–1725

Qin N, Baehr W (1994) Expression and mutagenesis of mouse rod photoreceptor cGMP phosphodiesterase. *J Biol Chem* **269:** 3265–3271

Read RJ (2001) Pushing the boundaries of molecular replacement with maximum likelihood. *Acta Crystallogr Section D Biol Crystallogr* **57:** 1373–1382

Skiba NP, Artemyev NO, Hamm HE (1992) The carboxyl terminus of the γ-subunit of rod cGMP phosphodiesterase contains distinct sites of interaction with the enzyme catalytic subunits and the α-subunit of transducin. *J Biol Chem* **270:** 13210–13215

Slep KC, Kercher MA, He W, Cowan CW, Wensel TG, Sigler PB (2001) Structural determinants for regulation of phosphodiesterase by a G protein at 2.0 A. *Nature* **409:** 1071–1077

Slepak VZ, Artemyev NO, Yun Z, Dumke CL, Sabacan L, Sondek J, Hamm HE, Bownds MD, Arshavsky VY (1995) An effector's site that stimulates G-protein GTPase in photoreceptors. *J Biol Chem* **270:** 14319–14324

Song J, Guo LW, Muradov H, Artemyev NO, Ruoho AE, Markley JL (2008) Intrinsically disordered γ-subunit of cGMP phosphodiesterase encodes functionally relevant transient secondary and tertiary structure. *Proc Natl Acad Sci USA* **105:** 1505–1510

Stockman A, Sharpe LT, Tufail A, Kell PD, Jeffery G (2006) Viagra slows the visual response to flicker. *Curr Biol* **16:** R44–R45, (2006)

Stockman A, Sharpe LT, Tufail A, Kell PD, Ripamonti C, Jeffery G (2007) The effect of sildenafil citrate (Viagra) on visual sensitivity. *J Vis* **7:** 1–15

Sung BJ, Hwang KY, Jeon YH, Lee JI, Heo YS, Kim JH, Moon J, Yoon JM, Hyun YL, Kim E, Eum SJ, Park SY, Lee JO, Lee TG, Ro S, Cho JM (2003) Structure of the catalytic domain of human phosphodiesterase 5 with bound drug molecules. *Nature* **425:** 98–102

Takemoto DJ, Hurt D, Oppert B., Cunnick J (1992) Domain mapping of the retinal cyclic GMP phosphodiesterase γ-subunit. *Biochem J* **281:** 637–643

Thaung C, West K, Clark BJ, McKie L, Morgan JE, Arnold K, Nolan PM, Peters J, Hunter AJ, Brown SD, Jackson IJ, Cross SH (2002) Novel ENU-induced eye mutations in the mouse: models for human eye disease. *Hum Mol Genet* **11:** 755–767

Tsang SH, Burns ME, Calvert PD, Gouras P, Baylor DA, Goff SP, Arshavsky VY (1998) Role for the target enzyme in deactivation of photoreceptor G protein *in vivo*. *Science* **282:** 117–121

Wang H, Liu Y, Huai Q, Cai J, Zoraghi R, Francis SH, Corbin JD, Robinson H, Xin Z, Lin G, Ke H (2006) Multiple conformations of phosphodiesterase-5: implications for enzyme function and drug development. *J Biol Chem* **281:** 21469–21479

Zhang KY, Card GL, Suzuki Y, Artis DR, Fong D, Gillette S, Hsieh D, Neiman J, West BL, Zhang C, Milburn MV, Kim SH, Schlessinger J, Bollag G (2004) A glutamine switch mechanism for nucleotide selectivity by phosphodiesterases. *Mol Cell* **215:** 279–286

Zhang X, Feng Q, Cote RH (2005) Efficacy and selectivity of phosphodiesterase-targeted drugs in inhibiting photoreceptor phosphodiesterase (PDE6) in retinal photoreceptors. *Invest Ophthalmol Vis Sci* **46:** 3060–3066

